JOURNAL OF SPACECRAFT AND ROCKETS
Vol. 44, No. 4, July–August 2007

Solar-Sail-Based Stopover Cyclers for Cargo Transportation Missions

Giovanni Mengali* and Alessandro A. Quarta†
University of Pisa, 56122 Pisa, Italy

DOI: 10.2514/1.24423

This paper addresses the problem of investigating promising options for cargo transportation in support of long duration robotic and human planetary missions. Because the propellant consumption plays a major role in these missions, we study stopover cyclers that use solar sails to connect the starting and the target planet periodically. To simplify the problem, circular and coplanar planetary orbits are assumed. Nevertheless, the real optical solar sail characteristics are taken into account and a comparison is established with respect to an ideal sail model. The advantages of stopover cyclers over classic cycler trajectories are obtained in terms of lower departure and arrival velocities, more flexibility in the design of the planet-centered orbit, and the elimination of the hyperbolic rendezvous without introducing propellant penalties. The feasibility of the proposed methodology is established by simulating stopover cyclers toward Mars, Venus, and Jupiter. A thorough investigation of the obtainable performance is given as a function of the solar sail optical parameters.

Nomenclature

A	=	sail area
$\boldsymbol{a}$	=	propulsive acceleration
b_1, b_2, b_3	=	force coefficients
c, d, e	=	best-fit approximation coefficients; see Eqs. (17) and (18)
k	=	integer multiple
m	=	sailcraft mass
n	=	cycler repeat time in synodic periods
$\hat{\boldsymbol{n}}$	=	unit vector normal to the sail
r	=	sun–spacecraft distance
$\hat{\boldsymbol{r}}$	=	sailcraft position unit vector
T_s	=	synodic period
t	=	time
α	=	pitch angle
β_σ	=	dimensionless sail loading
θ	=	polar angle
$\mu_\odot$	=	sun's gravitational parameter
σ_0	=	reference sail loading parameter
ω	=	angular velocity

Subscripts

min	=	minimum
p	=	payload
S	=	start planet
s	=	sail
T	=	target planet
t	=	time
θ	=	sweep angle
0	=	initial
1	=	end of S-T phase
2	=	end of T-T phase
3	=	end of T-S phase
4	=	end of S-S phase
$\oplus$	=	Earth
$\mathfrak{4}$	=	Jupiter
$\mathfrak{P}$	=	Mars
$\mathfrak{O}$	=	Venus

Superscript

$\star$	=	optimal

Introduction

THE renewed interest in solar system exploration for deepening our knowledge on the formation and evolution of planetary environment and for the search of new available resources [1–3] will require the implementation of sustained and affordable robotic and human programs [4]. To support these initiatives, a number of key building blocks are necessary. These include substantial testing of new approaches, systems, and operations, as well as the coordination of robotic elements and human and cargo transportation systems over the next few decades or more [5–8]. New missions call for the ability to transport significant payload across interplanetary distances in reasonable times and with a minimum expenditure of propellant and hardware to complete the mission. In situ planetary exploration system capabilities [9–11] also require the development of suitable infrastructures for mission support, to serve as a base for further missions and, ultimately, to reduce the total mission costs [12,13].

Cycler trajectories are characterized by periodical encounters between two planets without the need to stop at any of them [14,15]. Accordingly, cyclers have been proposed as a promising option for interplanetary transfers that require regular links between two planets [16], because of their inherent capability of propellant saving. In fact, cycler trajectories are predominantly ballistic in nature and typically require small adjustment maneuvers to be maintained continuously.

Most of the research studies have been concentrated on Earth–Mars cyclers [17–21]. In particular, the Aldrin cycler [22] and the Versatile International Station for Interplanetary Transport (VISIT) cyclers [23] have been deeply investigated, even if both of them present some drawbacks. For example, assuming a 15-year Earth–Mars cycler, the Aldrin cycler requires a not negligible cumulative ΔV for the corrective maneuvers (of the order of 1.5–2 km/s [15]), whereas VISIT cyclers have rather long revisit times (about five years, against 26 months of the Aldrin cycler [15]) and require large approach distances from the target (up to the radius of planet's sphere of influence). A possible solution to these problems has been proposed by Stevens and Ross who, recently, introduced the concept of solar-sail-based cyclers [24]. The rationale is that when the

Received 4 April 2006; revision received 5 December 2006; accepted for publication 18 December 2006.

*Associate Professor, Department of Aerospace Engineering; g.mengali@ing.unipi.it. Member AIAA.

†Research Assistant, Department of Aerospace Engineering; a.quarta@ing.unipi.it. Member AIAA.

momentum transfer of solar photons is used onto a large, lightweight, and reflective sail, the latter is propelled without the need of an active propulsion system or of any propellant. Nevertheless the cycler trajectories found by Stevens and Ross have the undesirable characteristic of high hyperbolic excess velocities at both departure and arrival, and require rendezvous and docking maneuvers on hyperbolic orbits. The aim of this paper is to overcome these problems by combining the use of solar sails with that of cyclers that stop at the planet and wait there until a new opportunity for returning back is opened. These trajectories are usually referred to as stopover cyclers [25–28].

Because propellant plays a major role in the cycler option, it is reasonable to investigate the opportunities offered by solar sails when faced with the time constraints introduced by the stopover cyclers. The improvements introduced in this paper with respect to the approach by Stevens and Ross [24] are given in terms of lower departure and arrival velocities, more flexibility in the design of the planet-centered orbit, and elimination of the hyperbolic rendezvous without any propellant penalty. Also, unlike Stevens and Ross, who assume an ideal sail reflection model, we study the effects of real optical sail coefficients on the overall cycler performance.

The paper is organized as follows: After a brief summary of the sail acceleration model, the stopover cycler is analyzed and the mission constraints are discussed. Assuming that the transfer phases between the starting and target planets (and vice versa) are traveled using a minimum time steering law, we investigate stopover cyclers toward Mars, Venus, and Jupiter as a function of the sail optical characteristics. The simulations emphasize the consistency of the proposed methodology.

Sail Acceleration Model

Before defining the main characteristics of the stopover cycler, it is useful to briefly recall the solar sail optical force model that is assumed throughout this paper. Instead of assuming an ideally reflecting surface, this model takes into account the optical coefficients of the real sail film. It was first proposed in the 1970s for solar sail trajectory optimization by Sauer [29] and further studied by Forward [30].

The propulsive acceleration of a flat solar sail, placed at a distance r from the sun, is [31]

$$\boldsymbol{a} = \frac{\beta_\sigma}{2}\frac{\mu_\odot}{r^2}\cos\alpha[b_1\hat{\boldsymbol{r}} + (b_2\cos\alpha + b_3)\hat{\boldsymbol{n}}] \tag{1}$$

where $\hat{\boldsymbol{n}}$ is in the direction of acceleration (shaded side of the sail), and $\alpha \triangleq \arccos(\hat{\boldsymbol{n}}\cdot\hat{\boldsymbol{r}})$. Also, $\beta_\sigma \triangleq \sigma_0/(m/A)$ [31] (where $\sigma_0 \triangleq 1.539\ \mathrm{g/m^2}$ [32]), whereas b_1, b_2, and b_3 are related to the thermooptical properties of the reflective film [33]. For a sail with a highly reflective aluminum-coated front side and a highly emissive chromium-coated back side, the force coefficients are [34] $b_1 = 0.1728$, $b_2 = 1.6544$, and $b_3 = -0.0109$. For an ideal sail with a perfectly reflective film, instead, the propulsive acceleration is directed along the unit vector $\hat{\boldsymbol{n}}$ and the force coefficients are $b_1 = b_3 = 0$ and $b_2 = 2$.

Cycler Analysis

In our analysis we consider direct transfers from a starting planet to a target planet. To simplify our discussion, and in accordance with the common practice [20], both the planets are assumed to cover circular and coplanar orbits (having radii r_S and r_T) with angular velocities $\omega_S = \sqrt{\mu_\odot/r_S^3}$ and $\omega_T = \sqrt{\mu_\odot/r_T^3}$, respectively.

At a generic time instant t the spacecraft position is defined, with respect to a polar inertial frame, through r and θ, the latter being measured counterclockwise from some reference position. At time t_0, when the first cycler starts, the polar angles $\theta_S(t_0) \triangleq \theta_{S_0}$ and $\theta_T(t_0) \triangleq \theta_{T_0}$ define the known azimuthal positions of the two planets.

A generic stopover cycler can be described through four phases. In the first one, referred to as S-T phase, the spacecraft is transferred from the starting to the target planet. The spacecraft then orbits around the target and waits for the next opportunity to return back. This waiting time at the target is denoted by T-T phase, whereas the return voyage towards the starting planet is called T-S phase. The stopover cycler ends with a waiting S-S phase at the starting planet, whose duration is equal to the time length necessary for the planets to return in the same relative configuration they occupied at time t_0. The main characteristics of these four phases are now thoroughly investigated.

S-T Phase

The maneuver in this phase starts at time t_0 when the spacecraft leaves the sphere of influence of the initial planet and ends at time t_1 when it reaches the target planet's sphere of influence. The time interval to complete this maneuver is referred to as $\Delta t_1 = t_1 - t_0$. It is assumed that the hyperbolic excess velocity with respect to both the planets is zero. This choice allows one to minimize the velocity variation necessary to transfer a given payload to the target planet. Under these assumptions, Δt_1 coincides with the time interval corresponding to a circle-to-circle orbit rendezvous.

Both the transfer time Δt_1 and the corresponding variation of the polar angle $\Delta\theta_1 = \theta_1 - \theta_0$ are a function of the steering law and of the solar sail performance (through the optical coefficients of the sail and the value of the dimensionless sail loading). In this paper we assume that Δt_1 coincides with the minimum feasible transfer time $\Delta t_1^\star$ and, therefore, that the sailcraft is transferred to the target planet as quickly as possible. The main reason comes from the necessity of reducing as much as possible the possibility that an onboard system failure represents a catastrophic event for the mission. In fact, during the transfer phase the sailcraft would be hardly reachable by a rescue mission, that, instead, could be carried out during the sailcraft orbiting phase around the target or the starting planet.

The condition $\Delta t_1 = \Delta t_1^\star$ amounts, on one side, to selecting the steering law for the pitch angle α (that, of course, coincides with the minimum transfer time steering law) and, on the other side, to establishing that the mutual position of the two planets at t_0 (that is, θ_{S_0} and θ_{T_0}) is such that an optimal rendezvous maneuver is feasible. The latter constraint on the initial planetary position is met through a suitable choice of the time t_0. Note that, having defined that the initial position of the starting planet is $\theta_{S_0} = 0$, the corresponding initial position of the target planet must satisfy the constraint

$$\theta_{T_0} = \Delta\theta_1^\star - \omega_T\Delta t_1^\star \tag{2}$$

As a consequence of the preceding assumptions, the minimum time interval $\Delta t_1^\star$ and the corresponding polar angle $\Delta\theta_1^\star$ swept by the sailcraft are functions of the performance characteristics of the sail only, that is,

$$\Delta t_1^\star = \Delta t_1^\star(b_1, b_2, b_3, \beta_\sigma) \tag{3}$$

$$\Delta\theta_1^\star = \Delta\theta_1^\star(b_1, b_2, b_3, \beta_\sigma) \tag{4}$$

The minimum time steering law $\alpha = \alpha^\star(t)$ that will be used in the simulations has been derived by Sauer using an ideal solar sail model [35] and, recently, by Mengali and Quarta for a nonperfect sail reflection model [34].

T-T Phase

In this phase the sailcraft orbits around the target planet for a time interval $\Delta t_2 = t_2 - t_1$ and waits for the opening of a return window. This waiting time can be used to transfer the payload from the sailcraft to the surface of the target planet.

From a practical viewpoint the heliocentric sailcraft orbit in this phase coincides with the orbit of the target planet. Accordingly, the corresponding polar distance travelled by the sailcraft is simply given by

$$\Delta\theta_2 = \omega_T\Delta t_2 \tag{5}$$

T-S Phase

The sailcraft performs the return travel towards the starting planet in a time interval $\Delta t_3 = t_3 - t_2$. As with the preceding S-T phase, we assume that the sailcraft hyperbolic excess velocity, at both the ends of this phase, is zero. Assuming, once again, that the transfer time is minimized (that is, $\Delta t_3 = \Delta t_3^\star$), for obvious symmetry reasons one has:

$$\Delta t_3^\star = \Delta t_1^\star \tag{6}$$

$$\Delta \theta_3^\star = \Delta \theta_1^\star \tag{7}$$

These relationships are in accordance with [36]. Their validity has been confirmed also by all of our numerical simulations.

Note that the assumption of transferring the sailcraft to the starting planet using a minimum time steering law amounts to specifying the relative position of the two planets at the time instant t_2. As explained later, this constraint is met through a suitable choice of the waiting time Δt_2.

S-S Phase

In this phase the sailcraft stands around the starting planet for a time interval $\Delta t_4 \triangleq t_3 - t_4$ and waits for the opening of a new launch opportunity towards the target planet. This waiting time can be used to stow a new payload and to perform the maintenance operations that are necessary to guarantee the effectiveness of the succeeding cycler. Like the T-T phase, the heliocentric sailcraft trajectory is assumed to coincide with the starting planet orbit. Accordingly, the sailcraft travels a polar distance given by

$$\Delta \theta_4 = \omega_S \Delta t_4 \tag{8}$$

Cycler Constraints for Repeatability

According to the four phases described in the preceding sections, the total cycler time $\Delta t \triangleq t_4 - t_0$ is obtained as

$$\Delta t = 2\Delta t_1^\star + \Delta t_2 + \Delta t_4 \tag{9}$$

whereas the total angular distance $\Delta\theta \triangleq \theta_4 - \theta_0$ traveled by the sailcraft in a whole cycler is [see Eqs. (5) and (8)]

$$\Delta\theta = 2\Delta\theta_1^\star + \Delta\theta_2 + \Delta\theta_4 = 2\Delta\theta_1^\star + \omega_T \Delta t_2 + \omega_S \Delta t_4 \tag{10}$$

Note that the time interval Δt_4 must be chosen so as to guarantee that at $t = t_4$ the relative positions of the sun, starting planet, and target planet are identical to their corresponding initial positions at $t = t_0$. This allows the cycler to be started again and the four phases to be repeated. From a mathematical standpoint, the latter requirement amounts to imposing the following two constraints. The first one is that Δt is an integer multiple n of the synodic period T_s of one planet with respect to the other [20], that is,

$$\Delta t = nT_s = \frac{2\pi n}{|\omega_S - \omega_T|} \tag{11}$$

From Eq. (11), n is referred to as cycler repeat time in synodic periods [20]. The second constraint involves the relative positions of the planets. In fact, the total angular distance traveled by the sailcraft minus the angular distance traveled by the starting planet must be equal to an integer multiple k of 2π, or

$$|\Delta\theta - \omega_S \Delta t| = 2k\pi \tag{12}$$

When Eqs. (9) and (10) are substituted into Eq. (12). one obtains

$$|2\Delta\theta_1^\star + \Delta t_2(\omega_T - \omega_S) - 2\omega_S \Delta t_1^\star| = 2k\pi \tag{13}$$

Equation (13) shows that the waiting time around the target planet depends on the sail performance characteristics and on the value of the integer k. Assume that k is chosen in such a way that

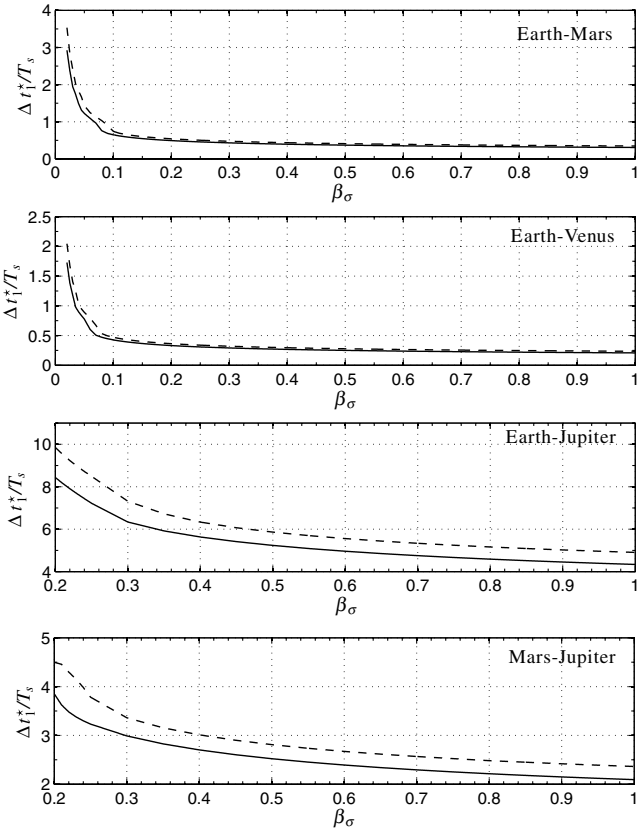

Fig. 1 Minimum transfer times $\Delta t_1^\star = \Delta t_3^\star$ for a sailcraft with ideal (solid line) and optical (dotted line) force model.

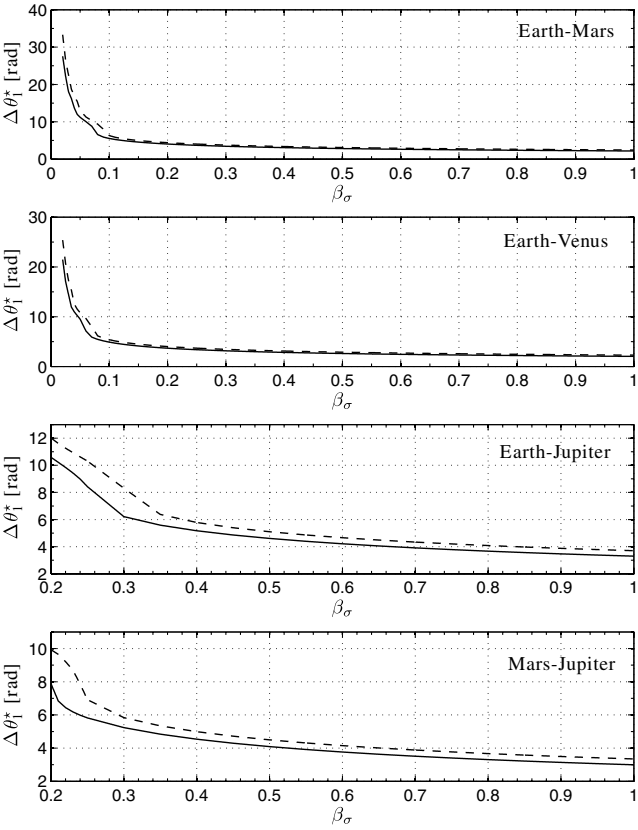

Fig. 2 Sweep angle $\Delta\theta_1^\star = \Delta\theta_3^\star$ for a sailcraft with ideal (solid line) and optical (dotted line) force model.

Table 1 Best-fit approximation coefficients of $\Delta t_1^\star$ and $\Delta\theta_1^\star$ [see Eqs. (17) and (18)]

Cycler	T_s, days	Sail force model	c_t	c_θ	d_t	d_θ	e_t	e_θ
Earth–Venus	584	Ideal	0.01573	0.2142	1.169	1.152	0.2115	2.085
		Optical	0.01994	0.2711	1.159	1.143	0.2244	2.159
Earth–Mars	780	Ideal	0.02786	0.2858	1.165	1.151	0.2963	2.078
		Optical	0.03663	0.3769	1.148	1.132	0.3099	2.09
Earth–Jupiter	399	Ideal	0.4638	0.4145	1.411	1.832	3.946	3.027
		Optical	0.4815	0.8049	1.51	1.545	4.471	2.873
Mars–Jupiter	816	Ideal	0.286	0.5176	1.167	1.357	1.846	2.627
		Optical	0.375	0.2096	1.583	2.16	4.551	3.358

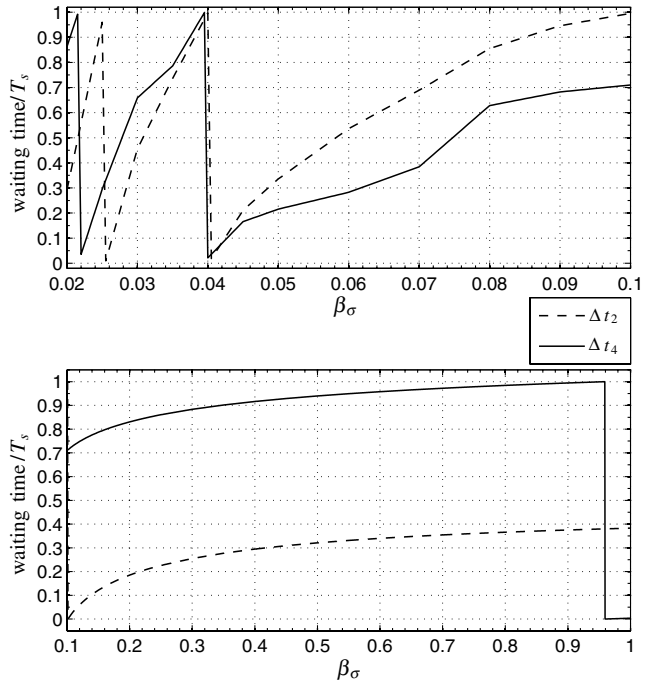

a) Ideal force model

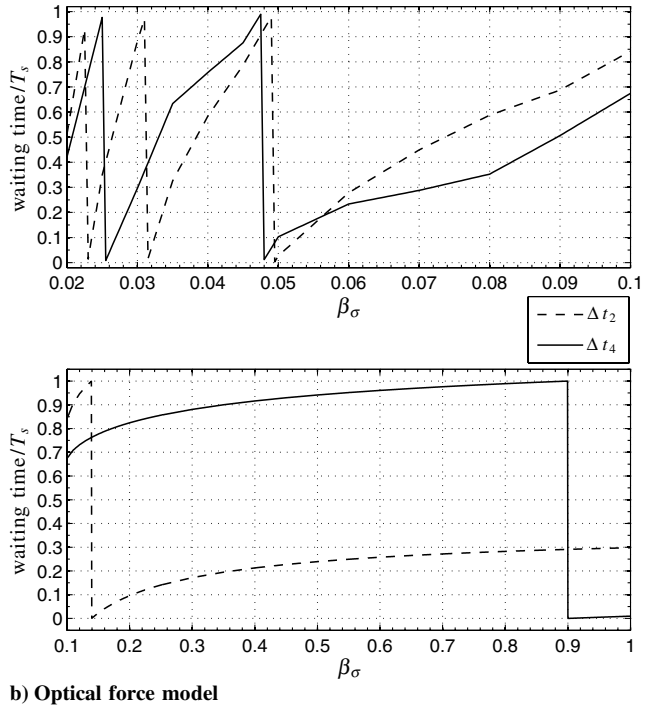

b) Optical force model

Fig. 3 Waiting times Δt_2 and Δt_4 for Earth–Mars stopover cyclers.

$$k \geq \left| \frac{\Delta\theta_1^\star}{\pi} - \frac{\omega_S}{\pi}\Delta t_1^\star \right| \tag{14}$$

and denote with $k_{\min}$ the least value of k that satisfies Eq. (14). Then, Eq. (13) can be written as

$$\Delta t_2 = kT_s + 2\frac{\Delta\theta_1^\star - \omega_S \Delta t_1^\star}{\omega_S - \omega_T} \tag{15}$$

A couple of remarks are in order. First, note that Δt_2 is positive (as is physically necessary), provided that Eq. (14) is met. Second, Eq. (15) is valid for both positive and negative values of $\omega_S - \omega_T$ [that is, Eq. (15) is able to model transfers for both inner and outer planets]. Because Δt_2 is an increasing function of k, in the following we will assume that $k = k_{\min}$ to minimize the time duration of the T-T phase.

Finally, recalling that $\Delta t_4 = \Delta t - 2\Delta t_1^\star - \Delta t_2$ [see Eq. (9)] and making use of Eq. (15), one obtains

$$\Delta t_2 = (n - k_{\min})T_s - 2\frac{\Delta\theta_1^\star - \omega_T \Delta t_1^\star}{\omega_S - \omega_T} \tag{16}$$

Because Δt_4 must be a nonnegative real number, Eq. (16) shows that n is constrained to satisfy a condition in the form $n \geq n_{\min}$, where $n_{\min}$ is the least value of n that allows the right side of Eq. (16) to take nonnegative values. Note that $n_{\min}$ plays a fundamental role in establishing the mission performance because, for a given sail configuration, it defines the minimum time interval necessary to complete the cycler [see Eq. (11)].

To summarize, a generic stopover cycler is fully characterized by the optical solar sail coefficients, by the dimensionless sail loading and by the values of n and k.

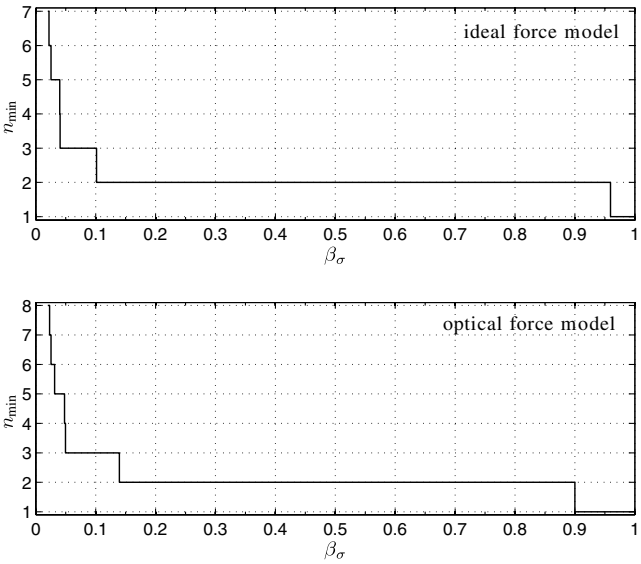

Fig. 4 Minimum cycler repeat time in synodic periods for an Earth–Mars mission.

Numerical Simulations

The performance of the stopover cyclers as described in earlier sections has been investigated for different combinations of start-target planets. In addition to the Earth–Mars cycler, which has found a considerable interest in the literature [19,21,37–39], we studied Earth–Venus, Earth–Jupiter, and Mars–Jupiter cyclers. The simulations have been performed both using an ideal sail model (with specular reflection characteristics) and a real set of sail film optical coefficients taken from [34].

The heliocentric orbits of all planets are assumed to be circular and coplanar. Their radii are $r_{\varsigma} = 0.72333199$ AU for Venus, $r_{\oplus} = 1$ AU for Earth, $r_{\sigma} = 1.523679342$ AU for Mars and $r_{\downarrow} = 5.20336301$ AU for Jupiter [40]. For Earth–Mars and Earth–Venus cyclers the dimensionless sail loading has been varied in the interval $\beta_\sigma \in [0.02, 1]$, whereas in the cyclers involving Jupiter the interval variation of β_σ has been narrowed to $[0.2, 1]$ for avoiding excessively long cycler times. Loosely speaking, a value $\beta_\sigma = 0.05$ corresponds to the limits of the current technology. A value $\beta_\sigma \cong 0.15$ will probably be available in the near future, whereas values greater than 0.5 are representative of very high-performance sails, such as those studied for Heliopause missions [41–43].

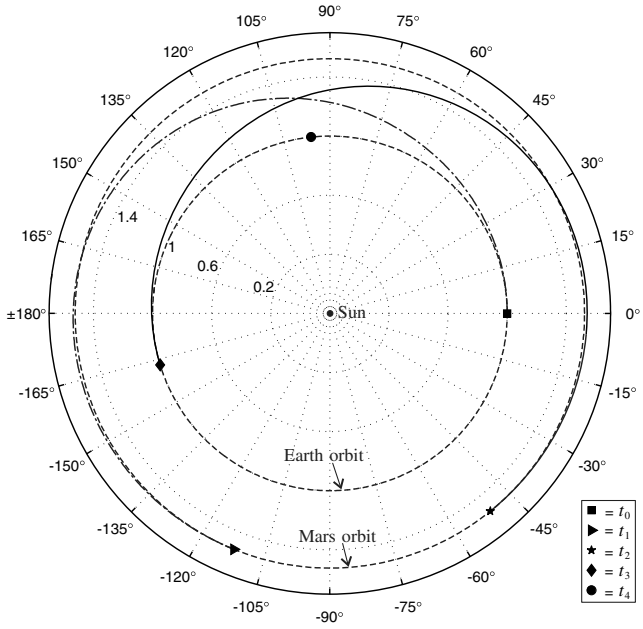

a) $\beta_\sigma = 0.17$, $n_{\min} = 2$

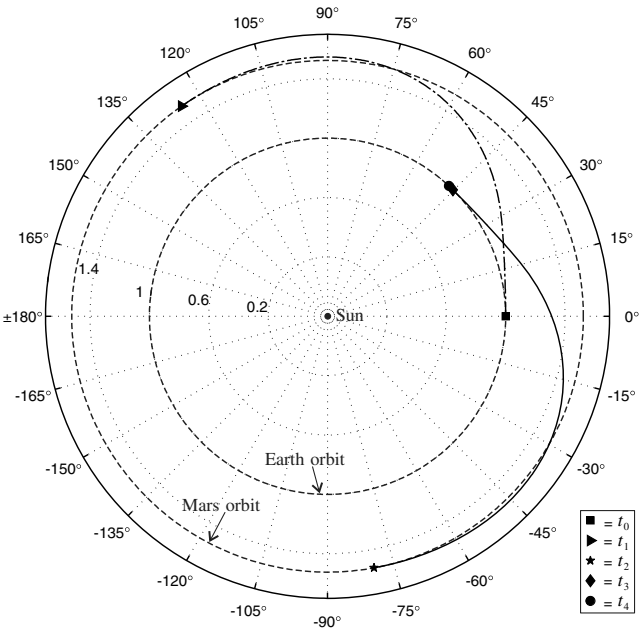

b) $\beta_\sigma = 1$, $n_{\min} = 1$

Fig. 5 Earth–Mars stopover cycler trajectory for a sailcraft with ideal force model.

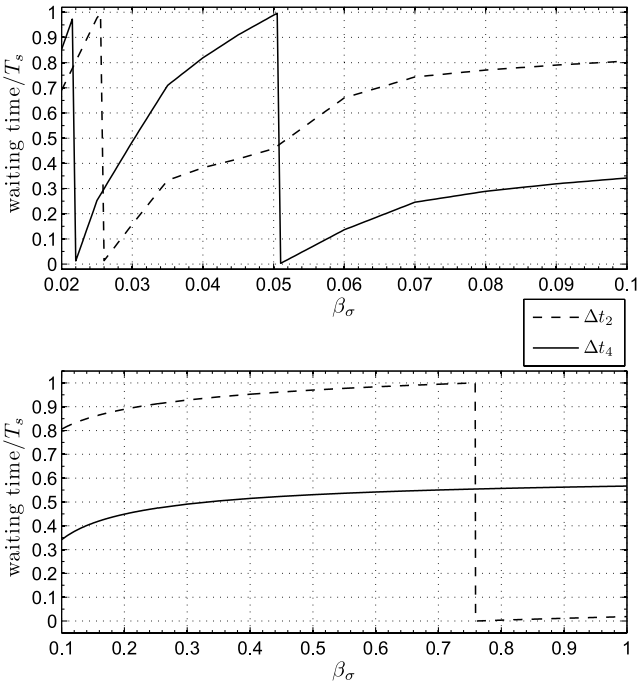

a) Ideal force model

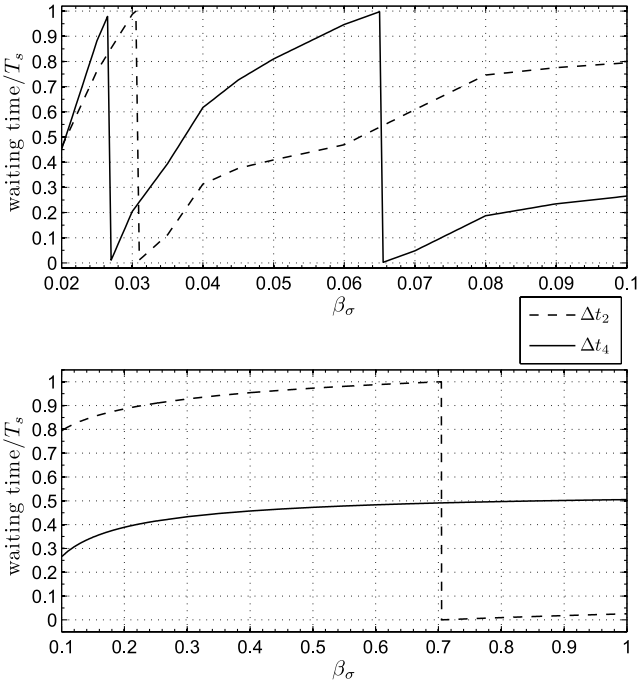

b) Optical force model

Fig. 6 Waiting times for Earth–Venus stopover cyclers.

The minimum transfer time $\Delta t_1^\star$ and the value of the sweep angle $\Delta\theta_1^\star$ are found by solving the corresponding optimal rendezvous problem between the two involved planets. The solution method, based on an indirect approach, employs a two-stage strategy that splits the optimization procedure in two steps: First, a genetic algorithm explores a large search space to obtain a rough estimate of the adjoint variables. Then, a combination of gradient-based and

direct methods are employed to refine the solution [34]. The results, obtained using a number of different values of the dimensionless sail loading, have been summarized in Figs. 1 and 2.

A two-term power series model in the form

$$\frac{\Delta t_1^\star}{T_s} = \frac{c_t}{(\beta_\sigma)^{d_t}} + e_t \tag{17}$$

$$\Delta\theta_1^\star = \frac{c_\theta}{(\beta_\sigma)^{d_\theta}} + e_\theta \tag{18}$$

is found to fit reasonably well the numerical data. The coefficients $c_{(t,\theta)}$, $d_{(t,\theta)}$, and $e_{(t,\theta)}$ have been obtained via nonlinear least-squares approximation and are shown in Table 1. Equations (17) and (18) give a maximum error on the order of 7% and can be used effectively to obtain a first estimate of the mission time and of the corresponding sweep angle.

Earth–Mars Stopover Cyclers

The results concerning the main characteristics (in terms of waiting times Δt_2 and Δt_4 and minimum cycler repeat time in synodic periods $n_{\min}$) of Earth–Mars stopover cyclers are shown in Figs. 3 and 4. Figure 4 shows that a stopover cycler with $n_{\min} = 1$, corresponding to a mission time length equal to the Earth–Mars synodic period ($T_s = 780$ days), is feasible only provided that very high-performance solar sails are employed, that is, sails having β_σ near to 1. Of course, in principle it would be possible to obtain cyclers with $n = 1$ and $\beta_\sigma < 1$. In that case, however, one should reduce (or even set to zero) the waiting time by introducing a penalty in terms of hyperbolic excess velocity different from zero at both ends of the transfer trajectory. This actually corresponds to defining cyclers that are identical to those analyzed by Stevens and Ross [24].

Recalling that the minimum mission time is proportional to $n_{\min}$, Fig. 4 also shows that a sail with an optical force model has an increased mission time (with respect to an ideal sail) for small values of β_σ and, instead, a decreased mission time for very high-performance sails. This seemingly surprising result is clarified by a comparison between Figs. 3 and 4. Note that the step jumps in $n_{\min}$ occur in correspondence of waiting times that take values equal to the synodic period T_s. In particular, as far as an optical solar sail model is concerned, Δt_4 approaches the synodic period for values of β_σ smaller than that for an ideal sail.

Figure 4 also shows the feasibility of obtaining stopover cycler with $n_{\min} = 2$ (both for ideal and optical solar sail models) for a rather large range of β_σ. As a result, a couple of sailcraft, deployed with a relative time delay equal to T_s, could in principle cover the Earth–Mars leg and release their payload with a frequency equal to the inverse of the synodic period.

Figure 5 shows the stopover cycler trajectory for a sailcraft with an ideal force model and two different values of the dimensionless sail loading, $\beta_\sigma = 0.17$ and $\beta_\sigma = 1$. The corresponding cycler repeat times in synodic period are $n_{\min} = 2$ and $n_{\min} = 1$, respectively (see Fig. 4). The first value, $\beta_\sigma = 0.17$, has been chosen for comparative purposes with the results obtained by Stevens and Ross [24]. In their analysis, Stevens and Ross (using $n = 1$) have found that the necessary hyperbolic excess velocity at departure is 2.53 km/s and at arrival is 4.30 km/s. On the other hand, the use of a stopover cycler allows one to set to zero both the hyperbolic excess velocities against a double required mission time (because $n_{\min} = 2$). However, note that the total cycler time obtained in [24], which is on the order of 26 months, is nearly identical to the minimum rendezvous time $\Delta t_1^\star + \Delta t_3^\star = 813$ days necessary to accomplish the S-T and T-S

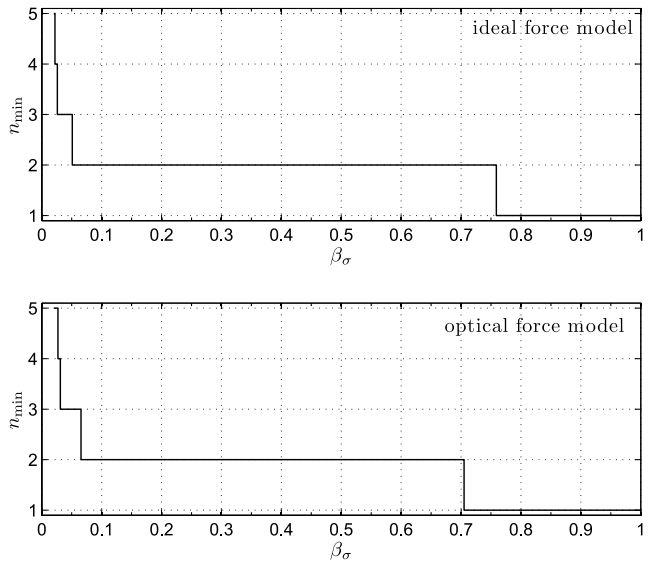

Fig. 7 Minimum cycler repeat time in synodic periods for an Earth–Venus mission.

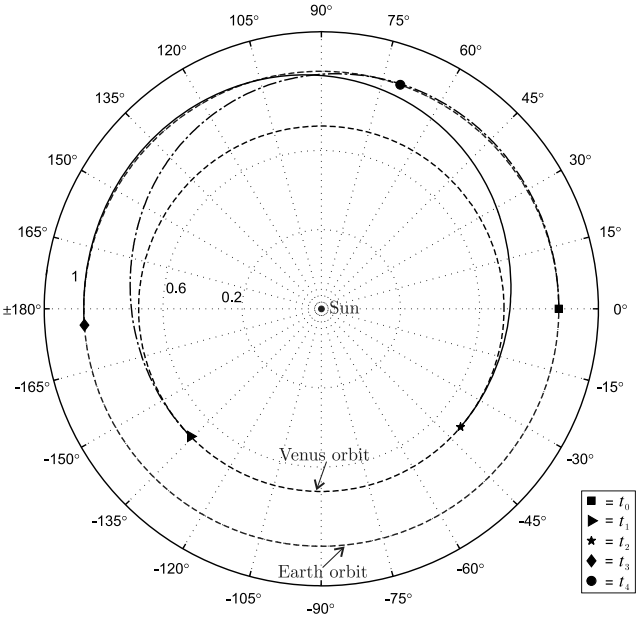

a) $\beta_\sigma = 0.17$, $n_{\min} = 2$

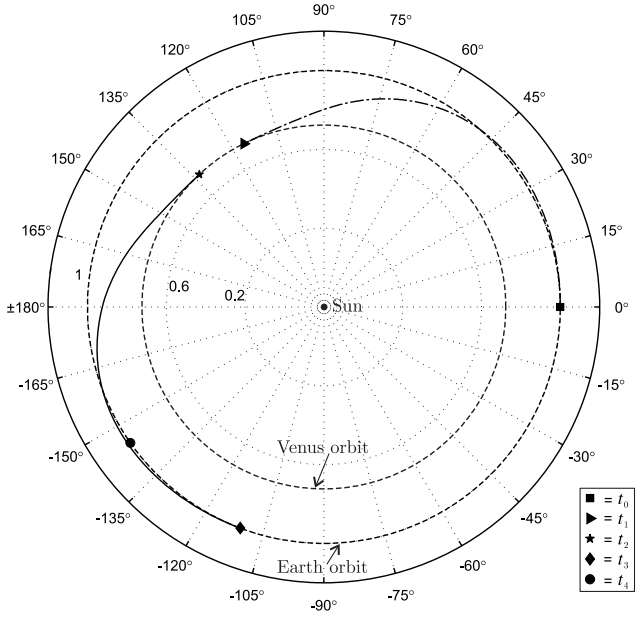

b) $\beta_\sigma = 1$, $n_{\min} = 1$

Fig. 8 Earth–Venus stopover cycler trajectory for a sailcraft with ideal force model.

phases. This means that the extra time required to complete a stopover cycler is passed by the sailcraft orbiting around the two planets.

Earth–Venus Stopover Cyclers

The results for Earth–Venus stopover cyclers are shown in Figs. 6 and 7. The results are qualitatively similar to those obtained for the Earth–Mars cyclers. The current or near-term technology allows one to obtain stopover cyclers with $n_{\min} = 2$, that is, 1168 days. The trajectories obtained for $\beta_\sigma = 0.17$ and $\beta_\sigma = 1$ are illustrated in Fig. 8.

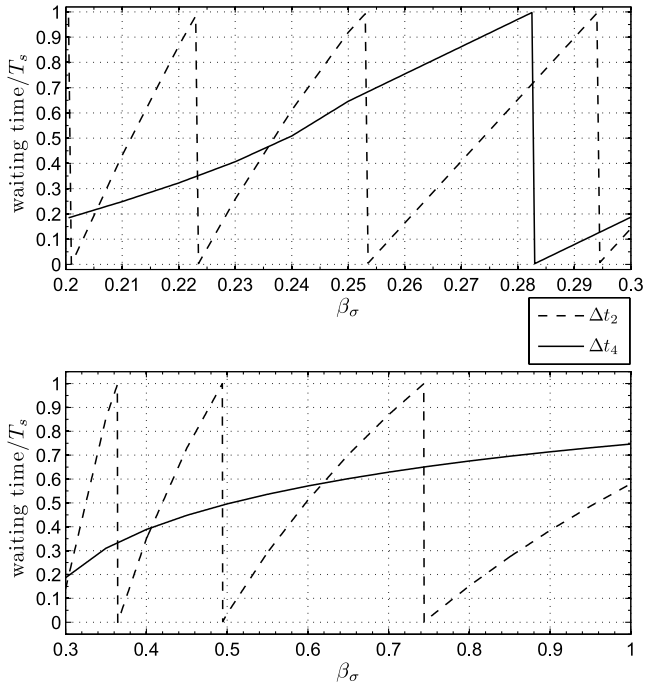

a) Ideal force model

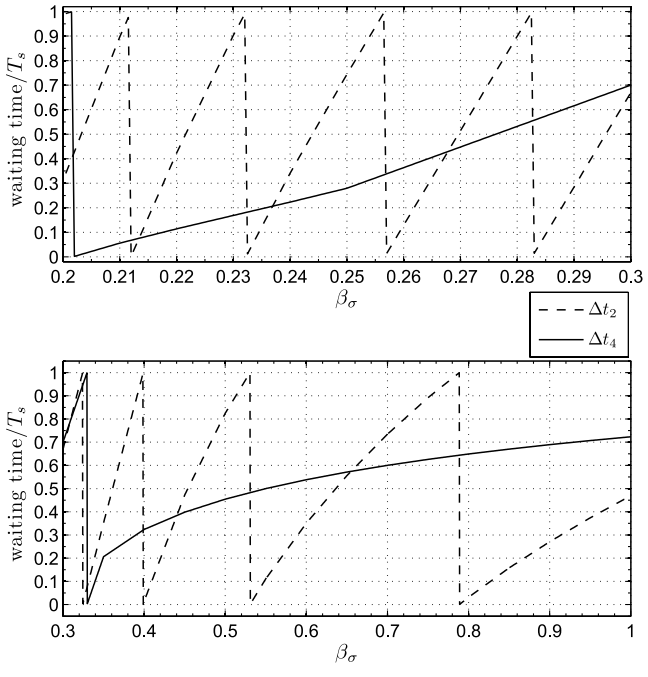

b) Optical force model

Fig. 9 Waiting times for Earth–Jupiter stopover cyclers.

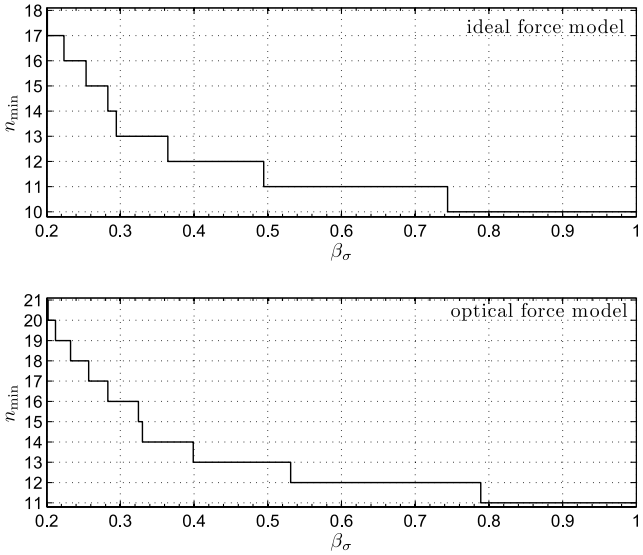

Fig. 10 Minimum cycler repeat time in synodic periods for an Earth–Jupiter mission.

Earth–Jupiter and Mars–Jupiter Stopover Cyclers

Finally, we present the results for Earth–Jupiter and Mars–Jupiter stopover cyclers. The unlimited availability of solar radiation pressure inside the solar system makes the use of solar sails attractive also for planning stopover cyclers toward outer planets, such as Jupiter. Because the solar radiation pressure decreases as the inverse square of the distance from the sun, the transfer times for missions toward outer planets are significant. This implies that the minimum total cycler times are on the order of 14 years (the corresponding transfer time being about 6.6 years) for optical solar sails with high performance ($\beta_\sigma \simeq 0.4$) and on the order of 12 years (and a transfer time of 5.5 years) for very high-performance sails ($\beta_\sigma \simeq 1$). The results are shown in Figs. 9 and 10.

It is interesting to compare the results for Earth–Jupiter with Mars–Jupiter stopover cyclers (see Figs. 11 and 12). The latter case is representative of a scenario in which a Martian base is exploited as a link for the study of the outer solar system. Figure 13 shows that the Mars–Jupiter total cycler times are typically longer, despite the

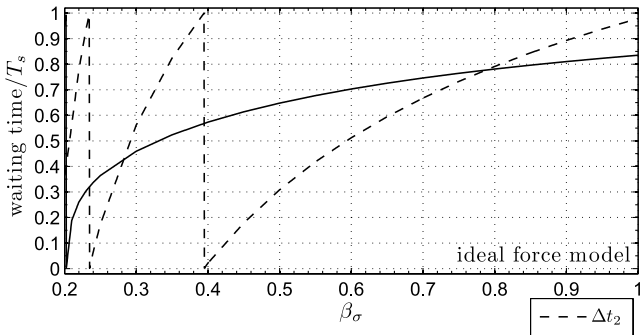

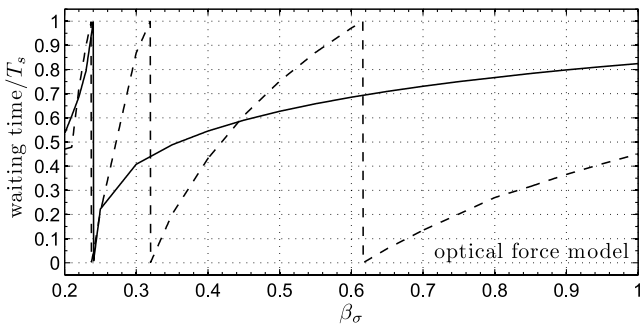

Fig. 11 Waiting times for Mars–Jupiter stopover cyclers.

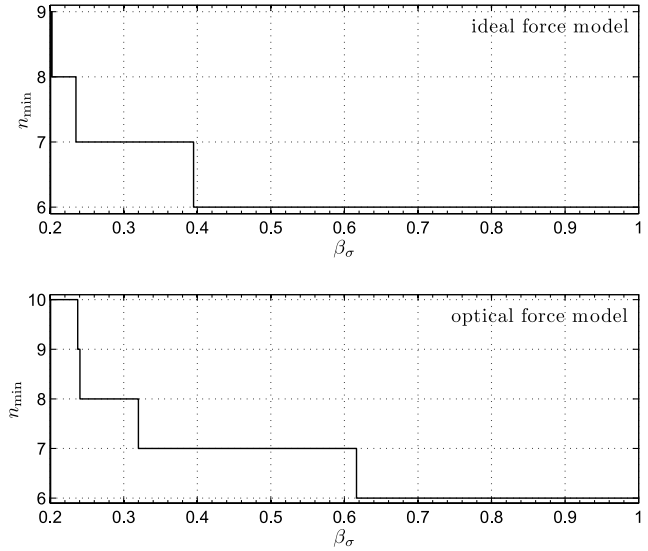

Fig. 12 Minimum cycler repeat time in synodic periods for a Mars–Jupiter mission.

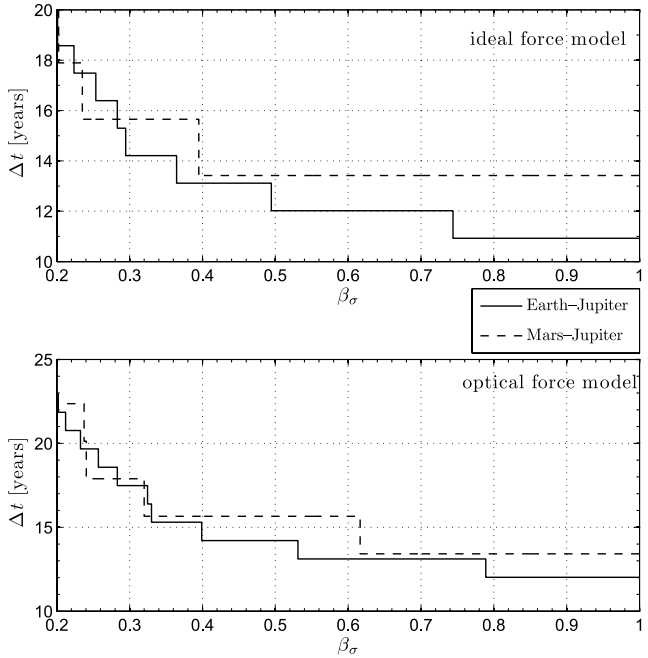

Fig. 13 Comparison of total mission times for Earth–Jupiter and Mars–Jupiter stopover cyclers.

shorter distance between the starting and target planets. The reason depends on two main elements: on one side the Earth–Jupiter synodic period is shorter than the Mars–Jupiter one, thus giving a heavier penalty in terms of waiting times around the two planets. On the other side, the mean propelling acceleration attainable during the Mars–Jupiter transfer is less than that in a Earth–Jupiter cycler.

Deliverable Payload Mass

An estimate of the deliverable payload mass can be obtained by partitioning the total mass of the spacecraft into two components, the sail film and structure mass m_s and the payload mass m_p, that is ,

$$m = m_s + m_p \tag{19}$$

Accordingly, the dimensionless sail loading can be written as

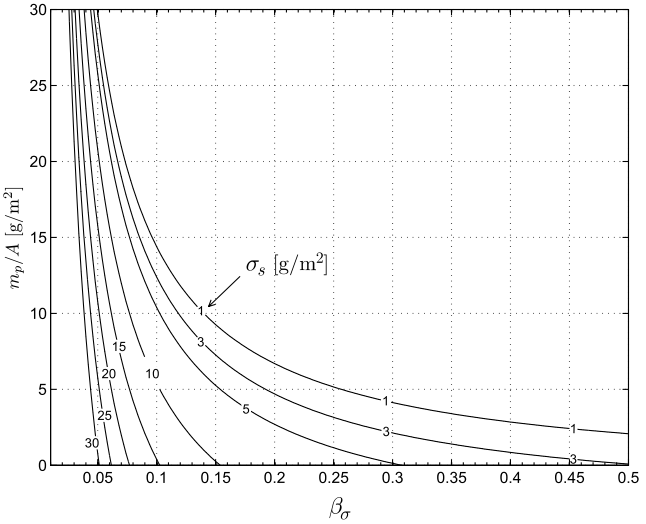

Fig. 14 Deliverable payload mass per unit area.

$$\beta_\sigma = \frac{\sigma_0}{\sigma_s + m_p/A} \tag{20}$$

where $\sigma_s \triangleq m_s/A$ is the sail assembly loading. Both β_σ and σ_s are technology parameters, based on the limits of the current (or future) sail technology [31]. In particular, σ_s is closely related to the value of the areal density of the sail film. Near-term demonstration missions are likely to have a sail assembly loading of order 25–30 g/m^2, even if midterm technology will probably allow values of 5–10 g/m^2. Future outer solar system missions will require an assembly loading of the order of 1 g/m^2.

Inverting Eq. (20), an expression for the deliverable payload mass per unit area is obtained as

$$\frac{m_p}{A} = \frac{\sigma_0}{\beta_\sigma} - \sigma_s \tag{21}$$

In other terms, for a fixed value of β_σ and σ_s, the deliverable payload mass per unit area is given. Its value is shown in Fig. 14 as a function of the available technology.

Conclusions

The performance of stopover cyclers using solar sails has been thoroughly investigated. Stopover cyclers are able to connect the starting and the target planet periodically and can be usefully employed for cargo transportation in support of long duration robotic and human planetary missions. Even if the obtained results are preliminary in the sense that the trajectories are assumed to be coplanar and the planet orbits circular, the real optical solar sail characteristics are taken into account and a comparison is established with respect to an ideal sail model. The simulations show the feasibility of the proposed methodology and emphasize interesting advantages over classic cycler trajectories. Significant edges are obtained in terms of lower departure and arrival velocities, more flexibility in the design of the planet-centered orbit, and the elimination of the hyperbolic rendezvous without the introduction of propellant penalties. A number of simulations have been performed with Mars, Venus, and Jupiter as target planets using a wide variation of the dimensionless sail loading parameter. The key point is that the mission time is not easily affected by changing the transfer speed over wide variations of the sail loading parameter. In fact, the transfer velocity does not change the total trip time except at discrete jumps where the time variation is a multiple of the synodic period between the starting and the target planet.

References

[1] Anon., "The Vision for Space Exploration," NASA, Feb. 2004, http://www.nasa.gov/pdf/55583main_vision_space_exploration2.pdf [cited 30 Nov. 2006].

[2] Hughes, P., Dennehy, C., Mosier, G., Smith, D., and Dallas, L., "GSFC Information Systems Technology Developments Supporting the Vision for Space Exploration," AIAA Paper 2004-6110, Sept. 2004.
[3] Saunders, R. S., "NASA's Solar System Exploration Program," AIAA Paper 2000-5324, Sept. 2000.
[4] Drake, B. G., Geffre, J., Derkowski, B., and Tripathi, A., "Technologies for Human Space Exploration: 'Earth's Neighborhood' and Beyond,"AIAA Paper 2001-4634, Aug. 2001.
[5] Spurlock, D., "Space Exploration Systems Integration," AIAA Paper 2005-2541, Jan.–Feb. 2005.
[6] Schier, J., and Rush, J., "Space Communication Architecture Supporting Exploration and Science: Plans & Studies for 2010-2030," AIAA Paper 2005-2517, Jan.–Feb. 2005.
[7] Talbot-Stern, J., "Design of an Integrated Mars Communication, Navigation and Sensing System," AIAA Paper 2000-11, Jan. 2000.
[8] McNutt, R. L., "Solar System Exploration: A Vision For the Next Hundred Years," IAC Paper 04-IAA.3.8.1.02, Oct. 2004.
[9] Chu, C., Hayat, S., and Udomkesmalee, S., "Mars Base Technology Program Overview," AIAA Paper 2005-6744, Aug.–Sept. 2005.
[10] Gale, A., and Edwards, R., "Requirements for Space Settlements on the Moon and Mars," AIAA Paper 2004-6033, Sept. 2004.
[11] Zubrin, R., Frankie, B., Muscatello, T., and Kito-Borsa, T., "Progress in the Development of Mars in Situ Propellant Production Systems," AIAA Paper 1999-855, Jan. 1999.
[12] Donahue, B. B., and Cupples, M. L., "Comparative Analysis of Current NASA Human Mars Mission Architectures," *Journal of Spacecraft and Rockets*, Vol. 38, No. 5, Sept.–Oct. 2001, pp. 745–751.
[13] Charania, A., "The Trillion Dollar Question: Anatomy of the Vision for Space Exploration Cost," AIAA Paper 2005-6637, Aug.–Sept. 2005.
[14] Ross, S., "A Systematic Approach to the Study of Non-Stop Interplanetary Round Trips," AAS Paper 63-007, Jan. 1963.
[15] Friedlander, A. L., Niehoff, J. C., Byrnes, D. V., and Longuski, J. M., "Circulating Transportation Orbits Between Earth and Mars," AIAA Paper 1986-2009, Aug. 1986.
[16] Landau, D., and Longuski, J., "A Reassessment of Trajectory Options for Human Missions to Mars," AIAA Paper 2004-5095, Aug. 2004.
[17] McConaghy, T. T., Landau, D. F., Yam, C. H., and Longuski, J. M., "Notable Two-Synodic-Period Earth-Mars Cycler," *Journal of Spacecraft and Rockets*, Vol. 43, No. 2, March–April 2006, pp. 456–465.
[18] McConaghy, T. T., Longuski, J. L., and Byrnes, D. V., "Analysis of a Class of Earth-Mars Cycler Trajectories," *Journal of Spacecraft and Rockets*, Vol. 41, No. 4, July–Aug. 2004, pp. 622–628.
[19] McConaghy, T. T., and Longuski, J. M., "Analysis of a Broad Class of Earth-Mars Cycler Trajectories," AIAA Paper 2002-4420, Aug. 2002.
[20] McConaghy, T. T., Russell, R. P., and Longuski, J. M., "Toward a Standard Nomenclature for Earth-Mars Cycler Trajectories," *Journal of Spacecraft and Rockets*, Vol. 42, No. 4, July–Aug. 2005, pp. 694–698.
[21] Byrnes, D. V., Longuski, J. M., and Aldrin, B., "Cycler Orbit Between Earth and Mars," *Journal of Spacecraft and Rockets*, Vol. 30, No. 3, May–June 1993, pp. 334–336.
[22] Aldrin, E. E., "Cyclic Trajectory Concepts," Science Applications International Corp., Aerospace Systems Group, Hermosa Beach, CA, Oct. 1985.
[23] Niehoff, J., *Pathways to Mars: New Trajectory Opportunities*, AAS Paper 86-172, July 1986.
[24] Stevens, R., and Ross, I. M., "Preliminary Design of Earth-Mars Cyclers Using Solar Sails," *Journal of Spacecraft and Rockets*, Vol. 42, No. 1, 2005, pp. 132–137.
[25] Ragsac, R. V., and Titus, R. R., "Optimization of Interplanetary Stopover Missions," *AIAA Journal*, Vol. 1, No. 8, Aug. 1963, pp. 1861–1864.
[26] Ragsac, R. V., "Two-Vehicle Mars Stopover with Rendezvous," *Journal of Spacecraft and Rockets*, Vol. 3, No. 6, June 1966, pp. 800–805.
[27] Chovit, A. R., and Kylstra, C. D., "Optimization of Manned Interplanetary Stopover Missions," AIAA Paper 1965-513, July 1965.
[28] Penzo, P., and Nock, K., "Earth-Mars Transportation Using Stop-Over Cyclers," AIAA Paper 2002-4424, Aug. 2002.
[29] Sauer, C. G., Jr., "A Comparison of Solar Sail and Ion Drive Trajectories for a Halley's Comet Rendezvous Mission,"AAS Paper 77-104, Sept. 1977.
[30] Forward, R., "Grey Solar Sails," *Journal of the Astronautical Sciences*, Vol. 38, No. 2, 1990, pp. 161–185.
[31] Dachwald, B., Mengali, G., Quarta, A. A., and MacDonald, M., "Parametric Model and Optimal Control of Solar Sails with Optical Degradation," *Journal of Guidance, Control, and Dynamics*, Vol. 29, No. 5, Sept.–Oct. 2006, pp. 1170–1178.
[32] McInnes, C. R., *Solar Sailing: Technology, Dynamics and Mission Applications*, Springer-Praxis Series in Space Science and Technology, Springer–Verlag, Berlin, 1999, p. 40.
[33] Wright, J. L., *Space Sailing*, Gordon and Breach Science Publishers, Philadelphia, 1992, pp. 227–233.
[34] Mengali, G., and Quarta, A. A., "Optimal Three-Dimensional Interplanetary Rendezvous Using Nonideal Solar Sail," *Journal of Guidance, Control, and Dynamics*, Vol. 28, No. 1, Jan.–Feb. 2005, pp. 173–177.
[35] Sauer, C. G., Jr., "Optimum Solar-Sail Interplanetary Trajectories," AIAA Paper 76-0792, Aug. 1976.
[36] McInnes, C. R., Hughes, G., and MacDonald, M., "Payload Mass Fraction Optimization for Solar Sail Cargo Missions," *Journal of Guidance, Control, and Dynamics*, Vol. 39, No. 6, 2002, pp. 933–935.
[37] Russell, R. P., and Ocampo, C. A., "Systematic Method for Constructing Earth-Mars Cyclers Using Free-Return Trajectories," *Journal of Guidance, Control, and Dynamics*, Vol. 27, No. 3, May–June 2004, pp. 321–335.
[38] Chen, K., Landau, D., McConaghy, T. T., Okutsu, M., and Longuski, J. M., "Preliminary Analysis and Design of Powered Earth-Mars Cycling Trajectories," AIAA Paper 2002-4422, Aug. 2002.
[39] Chen, K., McConaghy, T. T., Okutsu, M., and Longuski, J. M., "A Low-Thrust Version of the Aldrin Cycler," AIAA Paper 2002-4421, Aug. 2002.
[40] Seidelmann, K. P. (ed.), *Explanatory Supplement to the Astronomical Almanac*, University Science Books, Mill Valley, CA, 1992, p. 316, Table 5.8.1, Chap. 5.
[41] Sauer, C. G., Jr., "Solar Sail Trajectories for Solar Polar and Interstellar Probe Missions," AAS Paper 99-336, Aug. 1999.
[42] McInnes, C. R., "Mission Applications for High Performance Solar Sails," International Academy of Astronautics Paper IAA-L.98-1006, April–May 1998.
[43] McInnes, C. R., "Delivering Fast and Capable Missions to the Outer Solar System," *Advances in Space Research*, Vol. 34, No. 1, 2004, pp. 184–191.
[44] McInnes, C. R., "Payload Mass Fractions for Minimum-Time Trajectories of Flat and Compound Solar Sails," *Journal of Guidance, Control, and Dynamics*, Vol. 23, No. 6, 2000, pp. 1076–1078.

R. Braun
Associate Editor